Mechanobiological approaches to synthetic morphogenesis - learning by building

Marija Matejčić[1*] and Xavier Trepat[1,2,3,4*]

[1]Institute for Bioengineering of Catalonia (IBEC), The Barcelona Institute for Science and Technology (BIST), 08028 Barcelona, Spain.

[2]Facultat de Medicina, Universitat de Barcelona, 08036 Barcelona, Spain

[3]Institució Catalana de Recerca i Estudis Avançats (ICREA), Barcelona, Spain

[4]Centro de Investigación Biomédica en Red en Bioingeniería, Biomateriales y Nanomedicina (CIBER-BBN), 08028 Barcelona, Spain.

*Correspondence to:

Marija Matejčić, PhD
Institute for Bioengineering of Catalonia
Ed. Hèlix, Baldiri i Reixac, 15-21
Email: mmatejcic@ibecbarcelona.eu

Xavier Trepat, PhD
Institute for Bioengineering of Catalonia
Ed. Hèlix, Baldiri i Reixac, 15-21
Email: xtrepat@ibecbarcelona.eu

Keywords

Synthetic morphogenesis, tissue mechanics, tissue shape, tissue folding, cell dynamics.

Abstract

Tissue morphogenesis occurs in a complex physicochemical microenvironment of limited experimental accessibility. This often prevents a clear identification of the processes that govern the formation of a given functional shape. By applying state-of-the-art methods to minimal tissue systems, synthetic morphogenesis aims at engineering the discrete events that are necessary and sufficient to build specific tissue shapes. Here we review recent advances in synthetic morphogenesis, highlighting how a combination of microfabrication, optogenetics and mechanobiology is fostering our understanding of how tissues are built.

Highlights

- Advances in the field of epithelial tissue mechanics enable synthetic morphogenesis to build tissue systems whose mechanical properties can be controlled and measured.
- Canonical epithelial models, like MDCK cells, are being used to develop new devices to stretch and compress tissues or change tissue curvature.
- More recent tissue systems, like those based on iPSCs and organoids, are used in minimal setups to study tissue self-organization, like cell positioning and cell fate.
- Growing the same tissue in minimal 2D and 3D environments showed that the third spatial dimension is not required for some aspects of tissue self-organization.
- Synthetic substrates and protein patterning allow growing tissues with defined size and shape. Using stem cells, they were applied to demonstrate in a highly controlled way how initial tissue geometry and tissue mechanics affect the morphogenetic outcome.

Synthetic morphogenesis at the interface of engineered and self-organized tissues

The field of synthetic morphogenesis encompasses research in artificially building living structures of defined shapes. Rather than observing how living systems in vivo or in isolation self-assemble [1], synthetic morphogenesis guides these processes by tightly controlling properties like differentiation [2], positioning components [3] or mechanics [4,5]. Hence, it aims to identify the structural demands of developing tissues to ensure their stability and function, and examines their limits by, for example, changing size or shape [6–8]. On the other hand, the tools and model systems it uses may allow synthetic morphogenesis to build shapes that do not occur naturally or occur in diseased states [7]. Through this approach, alternative developmental paths can be investigated to be applied to regenerative medicine or engineering fields like soft robotics.

The term morphogenesis can be applied to many levels at which shape generation occurs, from protein folding to whole-body formation. In this review, we focus on the tissue scale that studies cell-driven morphogenesis of animal tissues. We exclude the fields of bioprinting (rev. in [9]) and organ-on-chip systems (rev. in [10–13]) that generally aim at complexity and application. Rather, we write about elementary systems and processes, with an emphasis on how mechanics enables shape control and tissue function in epithelia. As the field of tissue mechanics has boomed in the last decade or so [14,15], we think it is important to catalogue advances and identify major current and future challenges for combining tissue mechanics with synthetic morphogenesis, thus hopefully helping to focus community efforts.

Building elementary living shapes

Early studies attempted to artificially build living shapes by growing tissues on synthetic substrates that mimic natural morphology or releasing naturally occurring geometric constraints. Examples include the growth of bone tissue on a synthetic sponge [16] or the removal of the enveloping egg follicle to obtain spherical insect eggs from naturally elongated ones to study the effect of shape change on development [17]. Building on such early research, today's synthetic tissue morphogenesis lies at the intersection of developmental cell biology, bioengineering, materials science and physics (see Box I), employing powerful methods including biophysics tools, genetic modification, microscopy, detailed quantitative analyses and simulations.

Epithelial monolayers are the starting point of most synthetic morphogenesis studies (Figure 1). Their junctions and defined polarity allows them to be patterned [4,18,19], stretched [20,21] or compressed [22,23] to uncover basic mechanical features of tissue architecture and function, all important in order to control synthetic shapes. Typical studies in synthetic morphogenesis use established epithelial cell lines, like the dog kidney **MDCK** cells (e.g. [24]) and endothelial cells (e.g. [25]), or organ-specific culture, like colon epithelial cells [26]. More recently, studies began leveraging the power of animal stem cells, like **iPSC**s [27], **ESC**s [6] or ESC-like (see Glossary) populations [28] to study embryogenesis across the phylogenetic tree (rev. in [28,29]). Differentiated organoids or live tissue explants [30] can also be seeded on specialized substrates or devices to guide their growth and shaping. In the following sections, we discuss the latest strategies using a variation of cell types and substrates to build the elementary geometric structures that form during development of an organism, including sheets (Figure 1), spheres (Figure 2A-B), domes (Figure 2C) and tubes (Figure 2D-E).

Flat sheets

Although morphogenetic processes and the resulting shapes are typically thought about in three dimensions, studies demonstrated that many features integral to morphogenesis, such as tissue patterning, cell shape or force distribution, are recapitulated in flat tissue configurations (Figure 1B-D, rev. in [31]). Flat tissue layers generated from human ESCs (Figure 1B-B') recapitulate germ layer specification and are termed '2D gastruloids' [6], akin to their 3D counterparts [32]. Circular **ECM** (Matrigel) patterns reduce the geometrical heterogeneity of free growing colonies and guide differentiation of hESCs into three germ layers and trophoblast-like population. More specifically, tissue size controls the formation of gradients that direct germ layer differentiation, as BMP-4-based signaling gradient forms only in large enough human blastocyst colonies (radius 500 µm, but not 200 µm; [33]). Growing the same cells on triangular patterns [4] localized high tension to the triangle tips (Figure 1C-C'). At these points, mesoderm tissue was specified through canonical Wnt signaling, demonstrating that not only tissue size, but tissue shape as well play a role in germ layer differentiation. Given their strictly defined geometry, such patterned tissues can also be used to asses geometry-independent sources of heterogeneity in development [34].

Aside from gastrulation mechanisms, micropatterning methods were employed to study organ-specific development. Basics of human neurulation were recapitulated in 2D colonies of hESCs and hPSCs [35–37] and micropatterns were used as a base to grow a 3D tissue neurulation model (see Domes and [7]). Similarly to gastrulation, initial tissue shape and size was found to guide neural tube morphogenesis. Intestinal organoids also readily spread on flat substrates into enteroid monolayers or flat open-lumen organoids, and maintain the spatial organization and tissue patterning of the in vivo intestinal tissue. Growing such intestinal organoids on a thin Matrigel layer, an intrinsic WNT-BMP circuit was revealed to govern intestinal proliferation and organization [38]. On mechanically controllable substrates (**PAA** hydrogels), flat organoids were patterned into large (700-900 um) disks to standardize monolayer size (Figure 1D-D', [39]). They mapped cell-substrate traction forces, as well as tension that compartmentalizes the intestinal tissue and drives cell migration out of the crypt. In addition, by modulating substrate stiffness (PAA gels), they showed that the flat organoid retains the ability to generate 3D intestinal crypts, demonstrating that on soft (<1.5 kPa) substrates, the crypt region indented through apical constriction of the stem cells. A softer substrate results in more stem cells and a larger intestinal crypt [39,40].

Although 3D geometry can instruct cell differentiation and guide correct tissue organization based on curvature (see Figure 3, Engineering tissue folding and Cell migration), studies on morphogenesis in 2D show that not all morphogenetic processes require the third spatial dimension. For some investigations, like the ones outlined above, questions can be answered in more controllable, 2D patterned tissues.

Spheres

Lumenized spheres are organ precursors during development (e.g., otic vesicle), functional structures in adult organs (e.g., eyes or bladder) and undesired shapes in disease (e.g., polycystic kidney disease). Epithelia can be guided into spherical shapes by artificially confining cells (Figure 2A) or by enabling self-organization in mechanically defined substrates or on preformed molds (Figure 2B). In both cases, the lumen is typically apical, while the basal epithelial surface faces the environment. MDCK and human neural stem cells grown in spherical alginate shells ([41,42] respectively, Figure 2A-A') enclose an apical lumen and were used to study growth-mediated compression and buckling pressure of epithelia (see Figure 3B-B'', Buckling and [41]). In unconfined 3D cultures, many cell types ([43], [44]), including cancer cells [45], also self-assemble into spherical cysts. In intestinal organoids, a cystic shape is associated with a pluripotent stem cell state, devoid of differentiated cells, and differentiation implies budding out of the spherical structure. In this system, it was also discovered that Intestinal stem cells proliferate better on substrates of intermediate (1.3 kPa) stiffness, than on softer (300 Pa) substrates [46]. As stiffness influences cell survival, fate, as well as tissue shape, it should be controlled in synthetic morphogenesis projects by using mechanically well-defined substrates.

Aside from specific organs, like the intestine, embryogenesis of many animals is associated to a spherical shape. To study embryogenesis in synthetic systems, spherical structures reminiscent of early mammalian embryos, blastoids, were assembled in vitro (mouse: [47–49], human: [50–52], rev. in [53–55]; Figure 2B-B') and characterized as faithful models to study human implantation development [56,57]. In a microfluidic device, [57] blastoids from primed hESC clusters (Figure 2B') developed until the onset of gastrulation (i.e., primitive streak formation). With protocols to assemble embryonic structures and control their luminal pressure [58,59] in place, we can expect major advances in our knowledge of the mechanics of early human development.

Domes

Domes are curved, lumenized epithelial structures attached to a substrate [60,61] (Figure 2C-C'). They can be used to model lumen-filled in vivo organs like the healthy blastocyst or the otic vesicle, as well as diseased organs like the polycystic kidney, with more control than free-floating 3D spheres that we discussed above. Currently, dome generation success depends on cell type and relies on spontaneous cellular ion pumping.

Already in 1969, hemispherical blister-like structures were observed in MDCK monolayers [62]. These tissue domes form due to water influx basally, where ion concentration is higher because of cell pumping, altering osmotic pressure. Leveraging this phenomenon, the size and site of dome formation can be controlled by micropatterning ECM protein (fibronectin) on soft **PDMS** gels [60] to generate artificial domes with basal lumen formation due to localized detachment from the substrate. This synthetic system was used to discover that the MDCK epithelium adapts to extreme tissue strains that develop in a dome by allowing heterogeneous cell strains. At high tissue strains, some cells start exhibiting superelastic properties due to cortical dilution, allowing them to accommodate up to 10-fold increases in apical area. These large deformations do not damage the dome thanks to intermediate filaments, which act as a safety belt. This mechanism identified in a synthetic system was later established in vivo during drosophila gastrulation [63]. More recent studies also took advantage of closed-dome structures to map stresses on domes of different shapes [61] and built domes from human stem cells [7], with an elongated footprint to mimic the neural tube geometry. Here, stem cells seeded on rectangular patterns were covered with Matrigel and subsequently self-organized into a tissue bilayer. In time, a lumen opened between the layers, creating a tubular dome. Upon induction of neural cell fate by BMP4, a neural tube-like structure formed in the dome, surrounded by the domed non-neural ectoderm as in vivo. Here, the shape of the initial tissue affected the shape of the emerging neural tube. For example, a too wide tissue footprint resulted in two parallel indenting regions, rather than one, indicating that a strict initial geometry is essential for healthy development. This study demonstrates the power of in vitro morphogenesis to learn about processes and tissues typically hard to control, like human or post-implantation tissues of other mammals.

A point to keep in mind while studying domed structures is the polarity of the dome, i.e. whether the lumen is on the basal or on the apical side of the tissue. Aside from the blastocyst, most in vivo luminal tissues have apical lumens. In addition to most signaling hubs being localized apically, the apical and basal side of an epithelium also host different junctions, cytoskeletal and cortical elements, giving them different mechanical and mechanoresponsive properties [64]. Therefore, the same tissue with an apical or a basal lumen might require different luminal pressures, be differently pliable and respond differently to changes in shape (see Bending, Figure 1A’ and [5]).

In the future, we expect to see the dome architecture leveraged to create more systems in which luminal pressure can be controlled, as well as advances in theoretical modelling that will enable mechanical characterization of domed structures with different geometries (e.g. rectangular and round combined) or thicker domes (larger lateral surfaces), more reminiscent of developing in vivo tissues.

Tubes

Tissue tubes can originate from all three germ layers and build our respiratory, vascular, lymphatic, urinary, reproductive, neural and gastrointestinal systems. They are essential formations delivering products of most excretory tissues (e.g. pancreas, liver, mammary) to their target location, but also the starting points of development for some organs (e.g., heart, neural tube). In vivo and in vitro, tube-building endothelial cells respond to mechanical properties of their environment. These include transcriptional responses to ECM stiffness [65] or responses to fluid flow. For example, endothelial cells align in the direction of flow-generated shear stress [66], but tend to migrate against the flow [67]. In the zebrafish dorsal aorta, cell extrusion is mechanoresponsive and increased in conditions of abnormally low blood flow [68]

Engineering long tubular systems is typically linked to elastomeric (PDMS) structures, either fixed microfluidic devices (e.g., [25], Figure 2D) or deformable tubular shells [69,70] (Figure 2E). Seeded cells line these channels, akin to in vivo lumen ensheathment [71]. As the resulting tissue tube takes the shape and size of the confinement, these substrate configurations allow control over tube geometry and size. For example, deformable alginate tubes (Figure 2E'), [69] were used to control tube diameter as well as its curvature. By tracking the rate at which epithelia detached from the tube walls, researchers were able to rank two cell lines by contractility, with MDCK cells exhibiting higher contractility than mammary gland epithelial J3B1A cells. Premade channels, however, are not suitable for studies of lumen creation by more common mechanisms, such as cord hollowing or cavitation [72,73].

Critical advancements in our understanding of de novo lumen formation come from studying lumenization in organotypic cultures of spherical cysts (acini, e.g. [74], closed domes [75], rev. in [76]). When cysts of biliary epithelial cells are transferred from microwells into microfluidic channels, they open and line the channel to form tubular, partial bile duct-like structures [77]. To elongate a lumen in a formed tissue cord without breaking open a cyst, one can look for cues in vasculogenesis, i.e. the formation of the primary axial blood vessels, rather than the formation of higher order vessels (angiogenesis). In the zebrafish dorsal artery, lumens open up by a cord hollowing mechanism similar to lumens in cysts mentioned above, while in mouse, two distinct cord-like tissues fuse, maintaining a lumen in between [78]. Synthetic systems exploiting these mechanisms are still in their infancy, however. In a minimal system of two hepatocyte cells in a microwell [79], the lumen between them elongates towards minimal tension, formed by anisotropies in integrin adhesion and, consequently, intercellular tension and osmotic pressure. Synthetic anisotropic protein patterns might help to elongate lumens in larger cell groups, as well. In another study reminiscent of cord hollowing, covering micropatterned colonies of stem cells with ECM induced the separation of apical surfaces and consequent lumen opening (see Domes and [7]). It would be interesting to attempt to fuse multiple of such elongated domed lumens, by targeted protein patterning, fluid flow or by barrier removal, to extend tubular stem cell structures, and potentially differentiate them.

A possible avenue to increase complexity by more elaborate shapes lies in building epithelial branches and networks of epithelial tubes. Factors that drive branch development depend on tissue type and stage of network development, and consequently the role of mechanical factors here remain rather controversial [80]. Fluid flow is known to guide morphogenesis of lungs and kidneys [80–82], glands (rev. in [83]) and secondary vasculature (rev. In [84]). In the lung, the pattern of the surrounding muscle drives branch patterning [85], but in lung organoids, patterns are set by proliferative instabilities [86]. Synthetic systems investigating branching processes typically have a fixed network topology (rev. in [87]). However, some use **MMP**-

degradable substrates, natural or synthetic [88] ones, to investigate network remodeling. Combined with biophysical tools such as laser ablation, traction measurements or optogenetics, synthetic branching systems can have the potential to identify forces that define network topology and function [89,90], but also characterize previously unreported structures.

Engineering tissue folding

Morphogenesis throughout the animal kingdom depends on correctly generating epithelial folds in more basic shapes like the ones discussed at the beginning. Folds are precursors (imaginal discs, vertebrate heart, retina) or final functional structures (gyrencephalic brain, intestinal epithelium), but also appear as outgrowths in diseased states (pancreatic ductal cancer or colon polyps). In this section we discuss different approaches to engineer folds in elementary tissue shapes (Figure 3).

Scaffolding

Constant advances in microfabrication and material chemistry produced a myriad of biocompatible substrates (Box II) that can be shaped [91–94], degraded [95] or "programmed" [36,96–98] to have three-dimensional folds. After seeding cells on the prefolded substrate (Figure 3A), the tissue assumes the shape of this scaffold (Figure 3A'). This allows studies of the effect of curvature on cell type localization, cell differentiation, cell migration or overall tissue patterning, a phenomenon collectively referred to as curvotaxis [99]. MDCK cells in monolayers grown on undulating hydrogels (Figure 3A'') are thinner on top of 'hills' and thicker in 'valleys' [36], independent on scaffold wavelength. They seem to sense curvature through cell thickness, tissue density and nuclear shape and position, and respond by subsequent change in the localization of YAP (lower in high density regions), expression of nuclear lamins and proliferation rate. Cell localization within a migrating epithelial monolayer (leader vs. mid-cluster), as well as the size of the cell cluster [99] and curvature magnitude [100] all affect F-actin and nuclear positioning, excluding both from highly convex regions [100]. Longitudinal groove scaffolds also help orient monolayer growth [100]. The intestinal epithelium senses curvature, as well. Intestinal crypt-like regions of organoids preferentially localize in indented regions of the scaffold, while differentiated villus cells cover finger-like protrusions of the substrate [95]. Even though the 3D geometry is not necessary for crypt and villus compartmentalization [39], the scaffolding results indicate that curvature helps maintain the fixed localization of intestinal compartments. Biologically more complex scaffolds were created from a mesenchyme-like tissue made of precisely localized mesenchymal cell clusters covered by ECM [96]. The mesenchymal clusters compacted the ECM and introduced complex folds in the epithelium seeded on top, akin to folds in the intestine or avian skin.

Aside from folding the tissue by the substrate guiding its shape, folds can be generated by exploiting the tissue intrinsic forces to drive passive buckling (Figure 3B) or active bending (rev. in [101,102], Figure 3C), which we discuss below.

Buckling

Buckling is a passive deformation normal to the tissue plane that results from lateral compression (in plane of the epithelium) that occurs, for example, during confined growth of a tissue [103]. In vivo, buckling was suggested to drive specific stages of morphogenesis of teeth (germ invagination, [104]), brain (rev. in [105], mechanism is controversial), lung [86] and intestine (tube looping and villus formation, [106]), forming stable folds by releasing built-up compression (Figure 3B-B'). Synthetic buckling was achieved with proliferating MDCK monolayers grown inside a spherical confinement [41]. The tissue buckled basally under lateral compression, allowing the authors to report the buckling pressure of an epithelial monolayer to be ~100 Pa. Such a system allows testing of different confinement geometries (see Tubes) but does not allow precise control of compressive force. To investigate how epithelia respond to compressive strain without effects of the substrate, researchers work with suspended tissues [107]. In 2020, a suspended epithelium was used to identify ~-35% strain as the MDCK buckling threshold [108], which depends on tissue elasticity and pre-strain (Figure 3B''). Below this threshold, epithelia were able to accommodate the applied compression. A suspended tissue is a powerful technique but it can be applied only to cell types that form strong cell-cell junctions. In addition, to study epithelial invagination, i.e. buckling from the apical surface inwards, a pressure-based system ([5], see Bending) could be used to assess mechanical differences depending on fold direction, albeit it would need to be adapted to exert buckling-inducing forces.

Tissue thickness affects the mechanical properties of an epithelium and buckling is more common in thin structures, as many adult epithelia are. However, many developing tissues, like the vertebrate retina, brain or insect imaginal discs are thick, pseudostratified epithelia (>20 µm apico-basal axis, [109]) and require complementary destabilizing mechanisms to induce a bend prior to buckling. These include localized apical, basal or lateral cell constriction (see Bending), mitotic cell rounding [110] and cell death [111,112]. Currently, it is difficult to control buckling of thick tissues in vitro, as it is to grow such tissues in the first place. In vitro systems that self-organize into pseudostratified compartments, such as the open-lumen intestinal organoid with its pseudostratified crypt, might prove useful to study physics of more complex buckling phenomena.

Bending

To examine the effects of curvature change on the epithelium, pressure-based doming systems can be used [5]. An epithelial monolayer is grown on a thin elastic membrane suspended over a microfluidic channel. By applying positive or negative pressure in the channel, the epithelium was pulled inwards (smaller apical surface) or bulged outwards (smaller basal surface), thus assuming opposite curvatures. These different configurations trigger different propagation of Ca^{2+} waves and gene expression at the fold boundary, presumably through different mechanical stresses that cells experience with different shapes.

The introduction of localized bends in vivo, however, is a process typically driven by active changes in cell shape through apical [113], basal [114] or lateral [111,115,116] constriction (Figure 3C). Such processes in vitro can be driven both by tissue self-organization and extrinsic control. Open-lumen intestinal organoids mentioned above were shown to indent their crypts on soft substrates (<1.5 kPa, [39]) through self-organized apical constriction of stem cells. The same tissue was grown in light-degradable **PEG** substrates [95] and the substrate was locally softened, allowing the crypts to invaginate into the substrate in these softer regions. To manipulate such active tissue bending, in vivo studies genetically interfered with relevant transcription factors ([117,118]), used laser ablation ([119]) or optogenetics ([120]). In vitro, The CRY2/CIBN light dimerizer system was used in MDCK cells to activate RhoA with subcellular resolution using blue light [22]. Recently, OptoShroom3 was developed [121] (Figure 3C'') to allow light-induced constriction specifically of the apical cell surface in mammalian cells. With these tools, single-cell shape changes or tissue-wide folds can be introduced depending on the number of activated cells. Future studies should also look away from the apical surface, and into the morphogenetic potential of lateral and basal cell contraction to understand the mechanics of tissue bending and buckling.

Harnessing cell dynamics

In the previous sections we have discussed strategies to engineer elementary shapes and processes that build living tissues. Below, we describe how the ceaseless out-of-equilibrium dynamics of living cells, which direct natural morphogenetic processes, can be exploited during synthetic morphogenesis.

Topological defects

In active systems, orientation and topological defects entail very specific mechanical patterns. Defect sites have recently been identified as powerful localizers of morphogenetic processes, namely tissue organization in the mammalian liver [122] or body axis establishment in hydra [123] in vivo and 3D outgrowth from a monolayer in vitro [124,125]. Nematic order and topological defects may arise from supracellular actin cable orientation [123] or cell shape orientation [18,122,124,125]. In vitro, topological defects can be controlled by imposing geometrical/topological constraints (e.g. star [18] or disk [124]). It was shown in star-shaped tissue monolayers [18] that MDCK cell extrusion increased at +1/2 defects. Neural progenitor cells, on the other hand, accumulated and formed 3D mound at +1/2 defects and escaped from -1/2 defects [125] (Figure 4A). These differences might be due to cell type specifics, like the strength of cell adhesion. The same mechanisms might play a role in vivo, and guide morphogenesis in various systems. Overall, topological defects may not only shape tissues in vivo, but they can also help to predict and execute controlled morphogenetic processes in vitro.

Cell turnover

Cell extrusion and division are tightly regulated to maintain mechanical stress in a tissue during morphogenesis [126]. During synthetic morphogenesis, proliferation and extrusion can also be exploited as a building mechanism by, for example, inducing tissue compression or generating tissue flows. However, they also need to be well controlled or (pharmacologically) slowed down, if necessary, as cell turnover might destabilize the synthetic structure or create luminal obstruction by agglomerations of extruded cells. Studies already exploited proliferation as a morphogenetic mechanism in in vitro systems (e.g. [41]). Simple 2D setups were sufficient to suggest that outcomes might depend on cell type. In confined round monolayers, for example, proliferating myoblasts form 3D cell accumulations in the center of the monolayer island [124], while MDCK cells accumulate on the monolayer edge [127], creating a 3D cord-like structure with collective polarity. It is unclear how these different behaviors arise from different levels of cell-cell adhesion, traction, friction and contractility among different cell types.

Localized or differential proliferation drives many morphogenetic processes in vivo, such as the development of the vertebrate tooth or heart, or drosophila wing disc ([128–130], respectively). As a mechanoresponsive feature, proliferation could be also localized in vitro by controlling tissue shape [19], locally stretching/compressing on stretch systems [23] (Figure 4B), light-responsive hydrogels [131] or ferrogels [132], mixing clones that grow at different rates [133], or altering mechanical feedback that controls proliferation [133].

Compared to proliferation, cell extrusion has attracted less attention in synthetic systems but also holds a lot of potential to guide folding or control general tissue stresses, for example by locally increasing apico-basal force in the epithelium [111,112]. It can be mechanically triggered and localized similar to cell proliferation but with opposite effect of force application, and with the additional option of inducing extrusion through cell death, for example by laser ablation or UV-exposure. Together, control over cell proliferation and extrusion holds more potential than synthetic morphogenesis has exploited thus far.

Cell migration

In a system of guided morphogenesis, cell migration can be both a desired (e.g. gap closure, **EMT**) and undesired (destabilizing the structure or introducing defect) behavior. There are several ways in which mechanics can control migration. Most cell types (primer in [134]) migrate towards stiffer substrates (positive durotaxis, Figure 4C and [135]). However, some cell types (e.g., axons of retinal ganglion cells in Xenopus) follow different gradients, so the stiffness of the synthetic environment should be designed, but with cell type in mind. The same holds true for haptotaxis of adherent cells, where fibroblasts migrate towards regions with higher protein density more efficiently than mesenchymal stem cells [136]. Of note, ameboid cells like leukocytes were shown to follow opposite haptotactic gradients depending on the integrin ($\alpha 4\beta 1$ or $\alpha_L\beta_4$) used in their migration [137], opening a potential avenue for genetically altering epithelial cell migration, as well. Migration of some cell types can also be controlled by substrate curvature (curvotaxis, [99]), as well as fluid flow. In growing tubes of endothelial cells, cell migration would be necessary to grow and fuse tubes, and the direction of migration could be controlled by fluid flow direction [67] (rev. in [83]). In many cases, factors mentioned above also affect cell fate, a point to be considered especially while building structures of stem cells, where stemness-promoting factors can be used to mitigate differentiation and any associated mechanical and behavioral changes. In more recent developments, direct laser writing was applied on a synthetic substrate to create custom surfaces for endothelial cell migration [138] and optogenetics were used to direct cell migration of specific cells [139,140]. During synthetic morphogenesis, cell speed could potentially be finely controlled by combining the aforementioned approaches, like synthesizing substrates with different gradients of stiffness and ECM.

Concluding remarks

During development and disease, morphogenesis implies a combination of multiple shapes, like tubes and buds [141] and synthetic systems should be able to recapitulate these features while maintaining control and accessibility. We expect the most productive future avenues will address the outstanding challenges by incorporating next level ideas including 1) building more elaborate shapes and combining different shapes; 2) building shapes from multiple cell types and from different species (chimeras); 3) simultaneously controlling multiple cell behaviors, like contractility, adhesion, cell localization, cell differentiation, tissue growth rate or lumen formation; 4) controlling cell behavior in a cell type-specific manner; 5) rather than building by assembling, building by predictable collapse of 3D structures (see Outstanding questions box).

To highlight our engineering perspective on synthetic morphogenesis in this review, we grouped morphogenesis in discrete shapes and processes and discussed the experimental and mechanical aspect of building such elementary blocks. For an overview of top-down and bottom-up techniques to alter extracellular and cell-intrinsic mechanical properties in tissue engineering, we refer the reader to an excellent recent review [142]. For an open-source tool to compute traction forces, see [143] and for an in-depth overview of the latest developments to measure mechanical stress in tissues in 2D and 3D, [144].

Tissues in vivo depend on complex but precise mechanical and biochemical signals. Minimal systems, like epithelial monolayers on synthetic substrates, allow us to narrow down on the determinants of shape and function of organs. From the point of view of morphogenetic tissue mechanics, adding complexity to these systems is a clear aim, but should not be done at the expense of control and accessibility. Therefore, we encourage the development of mechanically controllable systems. By building from the bottom-up, we will slowly learn which cues are essential for which tissue and which living form.

Outstanding questions

- What are the limits of complexity that synthetic morphogenesis can rationally engineer?
- How can mechanical stresses be mapped and controlled in synthetic tissue structures?
- Which functional features depend on a 3D configuration, and which can be recapitulated in 2D and why?
- Can synthetic morphogenesis capture mechanochemical redundancies present in vivo?
- What is the minimal set of physical variables that need to be controlled to engineer multicellular morphogenetic processes?
- How can we combine synthetic generation of different shapes, like tubes and spheres, or branches and buds?
- Can we predict the mechanical stability of synthetic living structures based on cell type and shape?
- As complexity increases, what type of theoretical mechanical models will be needed to synthesize morphogenetic processes?
- Can we build shapes that do not occur naturally in 3D, perhaps with supernatural functionalities?

Acknowledgements

We thank the members of the Trepat, Roca-Cusachs and Arroyo laboratories for their discussions and support. This work was supported by: European Molecular Biology Organization (ALTF-1169 to M.M.), Generalitat de Catalunya (Agaur, SGR-2017-01602 to X.T.); Spanish Ministry for Science and Innovation MICCINN/FEDER (PGC2018-099645-B-I00 to X.T.); European Research Council (Adv-883739 to X.T.), Fundació la Marató de TV3 (project 201903-30-31-32 to X.T.); IBEC, IRB and CIMNE are recipients of a Severo Ochoa Award of Excellence from the MINECO; La Caixa Foundation (LCF/PR/HR20/52400004).

Declaration of Interests

The authors declare no competing interests.

Box I: Epithelial mechanics

The rational engineering of epithelial shapes requires an understanding (and eventually a measurement) of the state of mechanical stress at every point of the epithelial surface. As a first approximation, an epithelium can be considered as a flat or curved membrane that supports a 2D state of stress tangential to its surface. This approximation is valid when epithelial thickness is smaller than other relevant dimensions of the system (such as the lumen diameter) and when apico-basal tension asymmetries, bending moments or tissue spontaneous curvature can be neglected. The state of stress of the epithelium is then provided by a 2×2 matrix, called the stress tensor. Because this stress tensor is symmetric, at every point of the epithelium there exist two privileged directions, mutually orthogonal, along which stress is maximal and minimal, respectively.

For elementary geometries such as those discussed in section Building elementary living shapes, the stress tensor adopts a simplified form. In the case of sphere or a spherical dome of radius R, stress is uniform and isotropic, this is, it has the same value in every position and in every direction of the epithelium. The stress tensor then simplifies to a single scalar value, the epithelial surface tension σ, which is balanced by pressure in the lumen ΔP (Figure IA) and can be readily computed using Laplace's law:

$$\sigma = \frac{\Delta P}{2} R \qquad (1)$$

If epithelial shape deviates from a sphere but is symmetric about one axis, then the two principal stress directions are the circumferential and meridional directions (Figure IB). Tension along these directions can be computed as [145]:

$$\sigma_c = \frac{\Delta P}{2}\left(2 - \frac{R_c}{R_m}\right) \qquad (2)$$

$$\sigma_m = \frac{\Delta P}{2} R_c \qquad (3)$$

where σ_c and σ_m are stress values in the circumferential and meridional directions, respectively, and R_c and R_m are the local radii of curvature along those directions.

Besides luminal pressure and shape, the stress in the epithelium is also determined by the traction forces applied at the cell-substrate interface. For the case of a flat monolayer, mechanical equilibrium can be invoked to infer epithelial stress from the direct measurement of traction forces in a technology called monolayer stress microscopy [146]. For a curved monolayer, however, no method has yet been developed to generalize this approach.

In some morphogenetic processes, the membrane approximation discussed above is not applicable. This is the case of budding of the vertebrate intestinal crypt or ventral furrow formation during drosophila gastrulation, for example. In these processes, stresses normal to the epithelial surface are generated to drive out-of-plane deformations. One mechanism to generate out-of-plane stresses is an asymmetry between apical and basal contractility, which results in epithelial bending. Alternatively, out of plane stress can arise from buckling instabilities (see section Engineering tissue folding).

Box II: Homage to substrates

Mechanical properties of the tissue's environment play a crucial role in guiding morphogenesis by affecting cell contractility, migration, division, death, extrusion and differentiation. As substrates are in general easier to shape than tissues both in 2D and 3D, harnessing properties of the diverse available substrates in projects of synthetic morphogenesis makes possible the generation of more controlled structures. Substrates used in vitro include natural and synthetic substrates, that offer differing levels of control. Natural substrates include animal origins, like collagen or gelatine gels, commercial ECM extracts of mammalian tumors (Matrigel, Basement Membrane Extract, Geltrex) and animal free matrices (plant-based: Growdex, algal: alginate, bacterial: hyaluronic acid). ECMs of animal origin contain natural biochemical cues and protein structures and can be degraded by cells. However, the same properties are problematic, as degradability means substrate shape cannot be well controlled, biochemical cues are present at inconsistent amounts, and matrices have complex or unknown mechanical properties. Reducing the complexity of mechanical properties of natural substrates, a preprint [147] reports controlling viscoelasticity independent of substrate stiffness using alginate. Natural matrix stiffness is typically low, 10-300 Pa, which limits studies of durotaxis and production of stable structures. Increasing stiffness usually implies also increasing protein and growth factor concertation. However, collagen gels can be made stiffer, and their compressive modulus can be decoupled from protein content, for example by glycation [148] (rev. in [149]) and its stiffness can increase up to 6 kPa when methacrylated (**GelMA**).

Synthetic substrates mitigate the complexity of natural substrates and include glass, plastic, PAA, soft PDMS, NuSil PDMS, PEG, **PEGDA-AA**, PEG with functional additions and **NOA**. They have also been adapted to be artificially degradable and deformable [150]. To control tissue size and shape and cell adhesion, (synthetic) substrates are usually functionalized. Their surface can be micropatterned, which implies that extracellular matrix proteins (collagens, laminins, fibronectin etc., depending on cell type) are bound to a (2D) substrate in a defined spatial pattern and size, such as circular, triangular, square or rings. Proteins can be patterned using physical transfers from 3D stamps that carry the pattern (µ-contact printing) or through contactless methods that expose protein binding molecules only on the pattern (UV through patterned masks or digitally guided, maskless light exposure (PRIMO). Contactless patterning systems also allow creation of protein gradients, while multiprotein patterns can in principle be generated by both approaches. However, protocols for such more complex patterning are still not widely used due to the extensive optimization required for different proteins and substrates. In addition to surface functionalization, substrate bulk can be functionalized with coated beads that serve as a growth factor/signaling source and with micro and nano fluorospheres to track substrate deformation and measure cell-substrate traction forces.

Glossary

- ECM: Extracellular matrix, a network of proteins like collagen, laminin or fibronectin, building the protein stromal meshwork to which cells attach and through which they migrate. ECM composition, organization and stiffness affects cells, e.g. behavior and fate. Commercial sources include Matrigel and Basement Membrane Extract (BME).
- EMT: Epithelial-to-mesenchymal transition, a process of epithelial cells losing epithelial characteristics like cell polarity, and adhesion to neighbor cells. Cells acquire a migratory and/or invasive behavior. EMT is a hallmark of developmental and homeostatic processes, as well as of initiation of cancer metastases.
- ESC: Embryonic stem cell, pluripotent cells isolated from preimplantation embryos. They have the potential to differentiate into all three embryonic germ layers and their derivatives.
- GelMA: Gelatin methacryloyl. A modified gelatin (hydrolyzed and denatured collagen) hydrogel produced through the reaction of gelatin with methacrylic anhydride (MA), photocrosslinked (UV). As a tissue substrate it can be degraded and bound by cells, as the MMP and RGD sequences are preserved.
- HUVEC: Human umbilical vein endothelial cells, a human cell line widely used to study the formation and development and pathology of blood or lymphatic vessels. HUVECs originate from the endothelium of the umbilical cord.
- MDCK: Madin-Darby canine kidney epithelial cells, a mammalian cell line, widely used in biomedical and biophysical research. MDCK originate from a kidney tubule of a dog.
- MMP: Matrix metalloprotease, calcium-dependent protease degrading ECM proteins. They are also able to degrade other molecules, like specific cell surface receptors.
- NOA: Norland Optical Adhesive, a clear, colorless, liquid photopolymer that will cure when exposed to ultraviolet light.
- PAA: Polyacrylamide, a hydrogel used in tissue mechanics research to fabricate custom cell substrates of varying stiffness (0.3-300 kPa). Fluorescent microspheres can be incorporated in its bulk to track gel displacements and calculate cell-substrate traction forces.

- PDMS: Polydimethylsiloxane, a silicone-based organic polymer used in tissue mechanics research to fabricate custom cell substrates, including microfluidic channels. Fluorescent microspheres can be attached onto its surface to track gel displacements and calculate cell-substrate traction forces.
- PEG: Polyethylene glycol, a hydrogel used in tissue mechanics research to fabricate custom cell substrates. Can be prepared to contain cell-binding motifs (RGD) in bulk or to be hydrolytically degraded by the cells' MMPs. Stiffness varies, 0.5–5 kPa for cell degradable crosslinkers or 20-500 kPa for non-degradable.
- PEGDA-AA: Polyethylene glycol diacrylate-acrylic acid, a hydrogel made from poly(ethylene glycol) diacrylate (PEGDA) and acrylic acid (AA). Used to fabricate substrates with custom topology and mesh size that allow diffusion and gradient formation with biochemical factors of choice.
- iPSC: Induced pluripotent stem cell, a type of pluripotent stem cell generated from differentiated somatic cells. Somatic cells can be converted into pluripotent stem cells using the four Yamanaka factors (transcription factors Myc, Oct3/4, Sox2 and Klf4).

Figure legends

Figure 1 Examples of flat epithelial monolayers to study mechanics of morphogenesis.

(A) Epithelial monolayers grown on flat natural or synthetic substrates can be patterned into desired shapes and size. This is achieved by patterning molecules that promote cell-substrate adhesion, such as specific ECM proteins, by different methods (see Box II). An epithelium growing on a rectangular pattern is shown. (A') A small region of an epithelial monolayer (dashed line in (A)), showing basic epithelial junctional organization that impacts epithelial shapes and the polarity of built structures. Cells are bound to each other by apical (adherens) junctions and lateral junctions (only apical shown), and they attach to the substrate at their basal side, through integrins. (B) A schematic representation of a flat model of gastrulation, gastruloid, with germ layer-like regions labelled. The correct organization of this tissue depends on monolayer size. (B') Fluorescence microscopy image of a hESC immunostaining corresponding to the scheme in (B). Adapted with permission from [6]. 2014. Scale bar 100 µm. (C) A schematic of a monolayer of hESCs grown on triangular patterns. High tension develops in triangle tips, triggering the expression of a live mesoderm reporter T(brachyury). (C') Fluorescence microscopy image of an hESC triangular monolayer 30 h after BMP4 addition, corresponding to the scheme in (C). Signal has been normalized 0-1. Adapted with permission from [4]. Scale bar 250 µm. (D) A schematic of a monolayer of mouse small intestinal organoids grown on circular patterns. Despite its 3D geometry in vivo, the intestinal epithelium compartmentalizes de novo into crypts and villi-like regions on flat, 2D substrates. (D') Fluorescence microscopy image of immunostained mouse intestinal organoid, with stem cells labelled in olfactomedin 4 (green) and differentiated cells with cytokeratin 20 (magenta). Corresponding to the scheme in (D). Adapted from [39]. Scale bar 200 µm.

Figure 2 Substrate configurations for 3D synthetic morphogenesis.

(A)-(C) Epithelial spheres. (A) A schematic of growing epithelial spheres in spherical confinements. The inner surface of these shells is typically coated with ECM proteins, promoting basal attachment, and resulting in an apical lumen in the centre. (A') Fluorescence microscopy image of a monolayer of MDCK cells growing basally attached to a spherical alginate shell. Cell membranes are labelled in red and the alginate in green. Corresponding to the scheme in (A). Adapted with permission from [24]. Scale bar 100 µm. (B) A schematic of growing epithelial spheres with the aid of microwells. These are typically low adhesion wells, promoting cell aggregation. (B') Brightfield image of a hPSCs cluster growing in an 80 µm Geltrex well embedded in a microfluidic device. These clusters undergo several landmark gastrulation-like events and can be used to study early stages of human post-implantation development. Corresponding to the scheme in (B). Adapted with permission from [57]. Scale bar 80 µm. See main text for additional examples. (C) A schematic of growing epithelial hemispheres as domes, with the aid of protein micropatterning (green) to create low adhesion areas in the monolayer. (C') Fluorescence microscopy image of a MDCK dome grown on a soft PDMS gel patterned with fibronectin. Corresponding to the scheme in (C). Adapted with permission from [60]. Scale bar 50 µm. (D)-(E) Epithelial tubes. (D) A schematic of growing epithelial tubes using a microfluidic channel. These channels can be produced with a desired shape and size, typically from PDMS, mounted on glass. (D') Fluorescence microscopy image of a **HUVEC** (endothelial cell) tube grown in a microfluidic channel. Corresponding to the scheme in (D). Adapted from [25]. Scale bar 100 µm. (E) A schematic of growing epithelial tubes using a microfluidic channel. These channels can be produced with a desired shape and size, typically from PDMS, mounted on glass. (E')

Fluorescence microscopy image of an MDCK tube grown in a deformable alginate channel. Corresponding to the scheme in (E). Adapted from [69]. Scale bar 100 µm.

Figure 3 Generating epithelial folds.

(A)-(A'') Using substrates with preformed folds. (A) Cells are seeded on top of the ECM coated substrate and after reaching confluency (A') assume the curvature determined by the substrate. (A'') MDCK cell monolayers grown on corrugated hydroxy-polyacrylamide with different wavelengths. Cells are thinner on top of substrate hills than in the bottom on valleys. Adapted with permission from [36]. Scale bar 10 µm. (B)-(B'') Inducing epithelial buckling to generate folds. (B) The monolayer is laterally compressed by confined growth, pre-stretch or acute lateral compression, increasing pressure and cell density in the tissue. (B') Past the point of buckling pressure, the buckling instability drives an out-of-plane deformation and fold generation. Detachment from the substrate, i.e. basal buckling is illustrated. (B'') Buckling of a compressed suspended MDCK monolayer. Adapted with permission from [108]. Scale bar 50 µm. (C-C'') Creating epithelial folds by localized cell constriction. Apical constriction is shown. (C) Apical actomyosin contractility is locally enhanced in a subset of cells in an epithelial monolayer (red) (C') The actomyosin network of the stimulated cells constricts, decreasing apical cell area and changing cell shape. The resulting wedge-shaped cells deform the monolayer, indenting it into the substrate. (C'') Folding of an MDCK colony expressing GFP-NShroom3-iLID. Blue rectangle marks the blue-light stimulated region. Adapted from [121]. Scale bar 50 µm.

Figure 4 Controlling cell dynamics.

(A)-(A') Sites of topological defects localize mechanical patterns that can drive morphogenetic processes. (A) Here illustrated is a +/1/2 defect in a monolayer of mouse neural progenitor cells, that blocks cell flow at the front point of the defect and (A') a consequent formation of a 3D mound at the defect site. Adapted from [125] (B)-(B') Cell turnover can be controlled in synthetic systems. (B) Stretching MDCK monolayers by 28% by stretching the underlying membrane substrate. (B') Stretch release induces overcrowding in the monolayer that peaks 0.5 h after release. Crowding induces cell extrusion to maintain homeostatic cell density. Extrusion rate peaks 2 h after stretch release. Adapted from [23]. (C)-(C') Cell migration can be controlled by exploiting mechanical cues for migration, such as substrate stiffness. (C) Cells were grown on PAA substrates with a gradient of stiffness [135], limited by a 500 µm stencil. (C') After stencil removal, cells migrated preferentially towards stiffer regions of the substrate, displaying positive durotaxis.

Figure I Stress diagrams in curved epithelial sheets modelled as thin membranes

(A) Pressure and stress tensor in a spherical epithelial sheet with a fully closed lumen. Stress is uniform and isotropic along the surface (surface tension σ) and balanced by pressure in the lumen ΔP (B) Pressure and stress tensor in an axisymmetric, non-spherical curved epithelium. Stress is distributed along two principal directions, the circumferential (tension σ_c) and meridional (tension σ_m).

References

1 Sasai, Y. (2013) Cytosystems dynamics in self-organization of tissue architecture. *Nat. 2013 4937432* 493, 318–326

2 Guye, P. *et al.* (2016) Genetically engineering self-organization of human pluripotent stem cells into a liver bud-like tissue using Gata6. *Nat. Commun. 2016 71* 7, 1–12

3 Johnson, H.E. *et al.* (2020) Optogenetic Rescue of a Patterning Mutant. *Curr. Biol.* 30, 3414-3424.e3

4 Muncie, J.M. *et al.* (2020) Mechanical Tension Promotes Formation of Gastrulation-like Nodes and Patterns Mesoderm Specification in Human Embryonic Stem Cells. *Dev. Cell* 55, 679-694.e11

5 Blonski, S. *et al.* (2021) Direction of epithelial folding defines impact of mechanical forces on epithelial state. *Dev. Cell* 56, 3222-3234.e6

6 Warmflash, A. *et al.* (2014) A method to recapitulate early embryonic spatial patterning in human embryonic stem cells. *Nat. Methods 2014 118* 11, 847–854

7 Karzbrun, E. *et al.* (2021) Human neural tube morphogenesis in vitro by geometric constraints. *Nat. 2021 5997884* 599, 268–272

8 Huang, C.-K. *et al.* Surface curvature and basal hydraulic stress induce spatial bias in cell extrusion. DOI: 10.1101/2022.04.01.486717

9 Ramadan, Q. and Zourob, M. (2021) 3D Bioprinting at the Frontier of Regenerative Medicine, Pharmaceutical, and Food Industries. *Front. Med. Technol.* 0, 25

10 Huh, D. *et al.* (2011) From 3D cell culture to organs-on-chips. *Trends Cell Biol.* 21, 745–754

11 Ronaldson-Bouchard, K. and Vunjak-Novakovic, G. (2018) Organs-on-a-Chip: A Fast Track for Engineered Human Tissues in Drug Development. *Cell Stem Cell* 22, 310–324

12 Tajeddin, A. and Mustafaoglu, N. (2021) Design and fabrication of organ-on-chips: Promises and challenges. *Micromachines* 12,

13 Ingber, D.E. (2022) Human organs-on-chips for disease modelling, drug development and personalized medicine. *Nat. Rev. Genet.* DOI: 10.1038/S41576-022-00466-9

14 Patwari, P. and Lee, R.T. (2008) Mechanical control of tissue morphogenesis. *Circ. Res.* 103, 234–243

15 Goodwin, K. and Nelson, C.M. (2021) Mechanics of Development. *Dev. Cell* 56, 240–250

16 Winter, G.D. and Simpson, B.J. (1969) Heterotopic bone formed in a synthetic sponge in the skin of young pigs. *Nature* 223, 88–90

17 Junquera, P. (1984) Oogenesis in a paedogenetic dipteran insect under normal conditions and after experimental elimination of the follicular epithelium : An ultrastructural study. *Wilhelm Roux's Arch. Dev. Biol.* 193, 197–204

18 Saw, T.B. *et al.* (2017) Topological defects in epithelia govern cell death and extrusion. *Nat. 2017 5447649* 544, 212–216

19 Nelson, C.M. *et al.* (2005) Emergent patterns of growth controlled by multicellular form and mechanics. *Proc. Natl. Acad. Sci. U. S. A.* 102, 11594–9

20 Benham-Pyle, B.W. *et al.* (2015) Mechanical strain induces E-cadherin-dependent Yap1 and β-catenin activation to drive cell cycle entry. *Science (80-.).* 348, 1024–1027

21 Streichan, S.J. *et al.* (2014) Spatial constraints control cell proliferation in tissues. *Proc. Natl. Acad. Sci. U. S. A.* 111, 5586–5591

22 Valon, L. *et al.* (2017) Optogenetic control of cellular forces and mechanotransduction. *Nat. Commun.* 8, 14396

23 Eisenhoffer, G.T. *et al.* (2012) Crowding induces live cell extrusion to maintain homeostatic cell numbers in epithelia. *Nature* 484, 546–549

24 Trushko, A. *et al.* (2020) Buckling of an Epithelium Growing under Spherical Confinement. *Dev. Cell* 54, 655-668.e6

25 Li, X. *et al.* (2015) In Vitro Recapitulation of Functional Microvessels for the Study of Endothelial Shear Response, Nitric Oxide and [Ca2+]i. *PLoS One* 10, e0126797

26 Shin, W. and Kim, H.J. (2022) 3D in vitro morphogenesis of human intestinal epithelium in a gut-on-a-chip or a hybrid chip with a cell culture insert. *Nat. Protoc. 2022* DOI: 10.1038/s41596-021-00674-3

27 Morgani, S.M. *et al.* (2018) Micropattern differentiation of mouse pluripotent stem cells recapitulates embryo regionalized cell fate patterning. *Elife* 7,

28 Anlas, K. and Trivedi, V. (2021) Studying evolution of the primary body axis in vivo and in vitro. *Elife* 10,

29 Moris, N. *et al.* (2020) Experimental embryology of gastrulation: pluripotent stem cells as a new model system. *Curr. Opin. Genet. Dev.* 64, 78–83

30 Nelson, C.M. *et al.* (2017) Microfluidic chest cavities reveal that transmural pressure controls the rate of lung development. *Development* 144, 4328–4335

31 Blin, G. (2021) Quantitative developmental biology in vitro using micropatterning. *Development* 148,

32 Van Den Brink, S.C. *et al.* (2014) Symmetry breaking, germ layer specification and axial organisation in aggregates of mouse embryonic stem cells. *Development* 141, 4231–4242

33 Deglincerti, A. *et al.* (2016) Self-organization of human embryonic stem cells on micropatterns. *Nat. Protoc. 2016 1111* 11, 2223–2232

34 Tewary, M. *et al.* (2019) High-throughput micropatterning platform reveals Nodal-dependent bisection of peri-gastrulation–associated versus preneurulation-associated fate patterning. *PLOS Biol.* 17, e3000081

35 Britton, G. *et al.* (2019) A novel self-organizing embryonic stem cell system reveals signaling logic underlying the patterning of human ectoderm. *Dev.* 146,

36 Luciano, M. *et al.* (2021) Cell monolayers sense curvature by exploiting active mechanics and nuclear mechanoadaptation. *Nat. Phys. 2021 1712* 17, 1382–1390

37 Knight, G.T. *et al.* (2018) Engineering induction of singular neural rosette emergence within hPSC-derived tissues. *Elife* 7,

38 Thorne, C.A. *et al.* (2018) Enteroid Monolayers Reveal an Autonomous WNT and BMP Circuit Controlling Intestinal Epithelial Growth and Organization. *Dev. Cell* 44, 624-

633.e4

39 Pérez-González, C. *et al.* (2021) Mechanical compartmentalization of the intestinal organoid enables crypt folding and collective cell migration. *Nat. Cell Biol.* 23, 745

40 He, S. *et al.* (2021) Stiffness Regulates Intestinal Stem Cell Fate. *bioRxiv* DOI: 10.1101/2021.03.15.435410

41 Trushko, A. *et al.* Buckling of epithelium growing under spherical confinement. DOI: 10.1101/513119

42 Alessandri, K. *et al.* (2016) A 3D printed microfluidic device for production of functionalized hydrogel microcapsules for culture and differentiation of human Neuronal Stem Cells (hNSC). *Lab Chip* 16, 1593–1604

43 Natsiou, D. *et al.* (2017) Generation of spheres from dental epithelial stem cells. *Front. Physiol.* 8, 7

44 Pastrana, E. *et al.* (2011) Eyes Wide Open: A Critical Review of Sphere-Formation as an Assay For Stem Cells. *Cell Stem Cell* 8, 486

45 Weiswald, L.B. *et al.* (2015) Spherical Cancer Models in Tumor Biology. *Neoplasia* 17, 1

46 Gjorevski, N. *et al.* (2016) Designer matrices for intestinal stem cell and organoid culture. *Nature* 539, 560–564

47 Rivron, N.C. *et al.* (2018) Blastocyst-like structures generated solely from stem cells. *Nat. 2018 5577703* 557, 106–111

48 Sozen, B. *et al.* (2019) Self-Organization of Mouse Stem Cells into an Extended Potential Blastoid. DOI: 10.1016/j.devcel.2019.11.014

49 Kime, C. *et al.* (2019) Induced 2C Expression and Implantation-Competent Blastocyst-like Cysts from Primed Pluripotent Stem Cells. *Stem Cell Reports* 13, 485

50 Liu, X. *et al.* (2021) Modelling human blastocysts by reprogramming fibroblasts into iBlastoids. *Nat. 2021 5917851* 591, 627–632

51 Yu, L. *et al.* (2021) Blastocyst-like structures generated from human pluripotent stem cells. *Nat. 2021 5917851* 591, 620–626

52 Sozen, B. *et al.* (2021) Reconstructing aspects of human embryogenesis with pluripotent stem cells. *Nat. Commun. 2021 121* 12, 1–13

53 Gupta, A. *et al.* (2021) Bioengineering in vitro models of embryonic development. *Stem Cell Reports* 16, 1104

54 Shahbazi, M.N. *et al.* (2019) Self-organization of stem cells into embryos: A window on early mammalian development. *Science (80-.).* 364, 948–951

55 Simunovic, M. and Brivanlou, A.H. (2017) Embryoids, organoids and gastruloids: New approaches to understanding embryogenesis. *Dev.* 144, 976–985

56 Kagawa, H. *et al.* (2021) Human blastoids model blastocyst development and implantation. *Nat. 2021 6017894* 601, 600–605

57 Zheng, Y. *et al.* (2020) A microfluidics-based stem cell model of early post-implantation human development. *Nat. Protoc. 2020 161* 16, 309–326

58 Chan, C.J. *et al.* (2019) Hydraulic control of mammalian embryo size and cell fate. *Nat.*

2019 5717763 571, 112–116

59 Dumortier, J.G. *et al.* (2019) Hydraulic fracturing and active coarsening position the lumen of the mouse blastocyst. *Science (80-.).* 365, 465–468

60 Latorre, E. *et al.* (2018) Active superelasticity in three-dimensional epithelia of controlled shape. *Nature* 563, 203–208

61 Marín-Llauradó, A. *et al.* (2022) Mapping mechanical stress in curved epithelia of designed size and shape. *bioRxiv* DOI: 10.1101/2022.05.03.490382

62 Leighton, J. *et al.* (1969) Secretory Activity and Oncogenicity of a Cell Line (MDCK) Derived from Canine Kidneyand. *Science (80-.).* 163, 472–473

63 Bhide, S. *et al.* (2021) Mechanical competition alters the cellular interpretation of an endogenous genetic program. *J. Cell Biol.* 220,

64 Badugu, A. and Käch, A. Independent apical and basal mechanical systems determine cell and tissue shape in the Drosophila wing disc. DOI: 10.1101/2020.04.10.036152

65 Frye, M. *et al.* (2018) Matrix stiffness controls lymphatic vessel formation through regulation of a GATA2-dependent transcriptional program. *Nat. Commun. 2018 91* 9, 1–16

66 Levesque, M.J. and Nerem, R.M. (1985) The Elongation and Orientation of Cultured Endothelial Cells in Response to Shear Stress. *J. Biomech. Eng.* 107, 341–347

67 Ostrowski, M.A. *et al.* (2014) Microvascular Endothelial Cells Migrate Upstream and Align Against the Shear Stress Field Created by Impinging Flow. *Biophys. J.* 106, 366–374

68 Campinho, P. *et al.* (2020) Blood Flow Limits Endothelial Cell Extrusion in the Zebrafish Dorsal Aorta. *Cell Rep.* 31,

69 Maechler, F.A. *et al.* (2019) Curvature-dependent constraints drive remodeling of epithelia. *J. Cell Sci.* 132,

70 Zhang, W. *et al.* (2016) Elastomeric free-form blood vessels for interconnecting organs on chip systems. *Lab Chip* 16, 1579–1586

71 Helker, C.S.M. *et al.* (2013) The zebrafish common cardinal veins develop by a novel mechanism: Lumen ensheathment. *Dev.* 140, 2776–2786

72 Hogan, B.M. and Schulte-Merker, S. (2017) How to Plumb a Pisces: Understanding Vascular Development and Disease Using Zebrafish Embryos. *Dev. Cell* 42, 567–583

73 Andrew, D.J. and Ewald, A.J. (2010) Morphogenesis of epithelial tubes: Insights into tube formation, elongation and elaboration. *Dev. Biol.* 341, 34

74 Bryant, D.M. *et al.* (2014) A Molecular Switch for the Orientation of Epithelial Cell Polarization. *Dev. Cell* 31, 171

75 Rodríguez-Fraticelli, A.E. *et al.* (2012) Cell confinement controls centrosome positioning and lumen initiation during epithelial morphogenesis. *J. Cell Biol.* 198, 1011

76 Debnath, J. and Brugge, J.S. (2005) Modelling glandular epithelial cancers in three-dimensional cultures. *Nat. Rev. Cancer 2005 59* 5, 675–688

77 Rizki-Safitri, A. *et al.* (2018) Efficient functional cyst formation of biliary epithelial cells using microwells for potential bile duct organisation in vitro. *Sci. Reports 2018 81* 8, 1–

78 Strilić, B. *et al.* (2009) The molecular basis of vascular lumen formation in the developing mouse aorta. *Dev. Cell* 17, 505–515

79 Li, Q. *et al.* (2016) Extracellular matrix scaffolding guides lumen elongation by inducing anisotropic intercellular mechanical tension. *Nat. Cell Biol. 2016 183* 18, 311–318

80 Lang, C. *et al.* (2021) Organ-Specific Branching Morphogenesis. *Front. Cell Dev. Biol.* 9, 1380

81 Palmer, M.A. *et al.* (2021) Stress ball morphogenesis: How the lizard builds its lung. *Sci. Adv.* 7,

82 Unbekandt, M. *et al.* (2008) Tracheal occlusion increases the rate of epithelial branching of embryonic mouse lung via the FGF10-FGFR2b-Sprouty2 pathway. *Mech. Dev.* 125, 314

83 Campinho, P. *et al.* (2020) Blood Flow Forces in Shaping the Vascular System: A Focus on Endothelial Cell Behavior. *Front. Physiol.* 11, 552

84 Navis, A. and Nelson, C.M. (2016) Pulling together: Tissue-generated forces that drive lumen morphogenesis. *Semin. Cell Dev. Biol.* 55, 139–147

85 Goodwin, K. *et al.* (2019) Smooth muscle differentiation shapes domain branches during mouse lung development. *Dev.* 146,

86 Varner, V.D. *et al.* (2015) Mechanically patterning the embryonic airway epithelium. *Proc. Natl. Acad. Sci. U. S. A.* 112, 9230–9235

87 Costa, L. *et al.* (2020) Microfluidics for Angiogenesis Research. *Adv. Exp. Med. Biol.* 1230, 97–119

88 Zanotelli, M.R. *et al.* (2016) Stable engineered vascular networks from human induced pluripotent stem cell-derived endothelial cells cultured in synthetic hydrogels. *Acta Biomater.* 35, 32–41

89 Goodwin, K. and Nelson, C.M. (2020) Branching morphogenesis. *Development* 147,

90 Vaeyens, M.M. *et al.* (2020) Matrix deformations around angiogenic sprouts correlate to sprout dynamics and suggest pulling activity. *Angiogenesis* 23, 315–324

91 Huang, C.-K. *et al.* (2022) Surface curvature and basal hydraulic stress induce spatial bias in cell extrusion. *bioRxiv* DOI: 10.1101/2022.04.01.486717

92 Gjorevski, N. *et al.* (2022) Tissue geometry drives deterministic organoid patterning. *Science (80-.).* 375,

93 Altay, G. *et al.* (2022) Modelling biochemical gradients in vitro to control cell compartmentalization in a microengineered 3D model of the intestinal epithelium. *bioRxiv* DOI: 10.1101/2021.12.13.472418

94 Altay, G. *et al.* (2020) Imaging the Cell Morphological Response to 3D Topography and Curvature in Engineered Intestinal Tissues. *Front. Bioeng. Biotechnol.* 8, 294

95 Gjorevski, N. *et al.* (2022) Tissue geometry drives deterministic organoid patterning. *Science (80-.).* 375,

96 Hughes, A.J. *et al.* (2018) Engineered Tissue Folding by Mechanical Compaction of the

Mesenchyme. *Dev. Cell* 44, 165-178.e6

97 Chen, T. *et al.* (2018) Combining 3D Printing with Electrospinning for Rapid Response and Enhanced Designability of Hydrogel Actuators. *Adv. Funct. Mater.* 28, 1800514

98 Kourouklis, A.P. and Nelson, C.M. (2018) Modeling branching morphogenesis using materials with programmable mechanical instabilities. *Curr. Opin. Biomed. Eng.* 6, 66–73

99 Pieuchot, L. *et al.* (2018) Curvotaxis directs cell migration through cell-scale curvature landscapes. *Nat. Commun. 2018 91* 9, 1–13

100 Rougerie, P. *et al.* (2020) Topographical curvature is sufficient to control epithelium elongation. *Sci. Rep.* 10,

101 Tozluoğlu, M. and Mao, Y. (2020) On folding morphogenesis, a mechanical problem. *Philos. Trans. R. Soc. B Biol. Sci.* 375, 20190564

102 Pearl, E.J. *et al.* Cellular systems for epithelial invagination. , *Philosophical Transactions of the Royal Society B: Biological Sciences*, 372. 19-May-(2017) , Royal Society

103 Nelson, C.M. (2016) On Buckling Morphogenesis. *J. Biomech. Eng.* 138, 0210051

104 Takigawa-Imamura, H. *et al.* (2015) Tooth germ invagination from cell–cell interaction: Working hypothesis on mechanical instability. *J. Theor. Biol.* 382, 284–291

105 Garcia, K.E. *et al.* (2018) Mechanics of cortical folding: stress, growth and stability. *Philos. Trans. R. Soc. B Biol. Sci.* 373,

106 Shyer, A.E. *et al.* (2013) Villification: How the gut gets its villi. *Science (80-.).* 342, 212–218

107 Harris, A.R. *et al.* (2013) Generating suspended cell monolayers for mechanobiological studies. *Nat. Protoc. 2013 812* 8, 2516–2530

108 Wyatt, T.P.J. *et al.* (2020) Actomyosin controls planarity and folding of epithelia in response to compression. *Nat. Mater.* 19, 109–117

109 Strzyz, P.J. *et al.* (2016) Heterogeneity, Cell Biology and Tissue Mechanics of Pseudostratified Epithelia: Coordination of Cell Divisions and Growth in Tightly Packed Tissues. In *International Review of Cell and Molecular Biology* 325pp. 89–118, Elsevier Inc.

110 Kondo, T. and Hayashi, S. (2013) Mitotic cell rounding accelerates epithelial invagination. *Nature* 494, 125–129

111 Monier, B. *et al.* (2015) Apico-basal forces exerted by apoptotic cells drive epithelium folding. *Nat. 2015 5187538* 518, 245–248

112 Roellig, D. *et al.* (2022) Force-generating apoptotic cells orchestrate avian neural tube bending. *Dev. Cell* 57, 707-718.e6

113 He, B. *et al.* (2014) Apical constriction drives tissue-scale hydrodynamic flow to mediate cell elongation. *Nature* 508, 392–396

114 Sidhaye, J. and Norden, C. (2017) Concerted action of neuroepithelial basal shrinkage and active epithelial migration ensures efficient optic cup morphogenesis. *Elife* 6,

115 Sui, L. and Dahmann, C. (2020) Increased lateral tension is sufficient for epithelial

folding in Drosophila. *Development* 147,

116 Gracia, M. *et al.* (2019) Mechanical impact of epithelial−mesenchymal transition on epithelial morphogenesis in Drosophila. *Nat. Commun.* 10,

117 Córdoba, S. and Estella, C. (2018) The transcription factor Dysfusion promotes fold and joint morphogenesis through regulation of Rho1. *PLOS Genet.* 14, e1007584

118 Leptin, M. (1991) twist and snail as positive and negative regulators during Drosophila mesoderm development. *Genes Dev.* 5, 1568–1576

119 Guo, H. *et al.* (2022) Optogenetic inhibition of actomyosin reveals mechanical bistability of the mesoderm epithelium during Drosophila mesoderm invagination. *Elife* 11,

120 De Renzis, S. (2020) Morphogenesis: Guiding Embryonic Development with Light. *Curr. Biol.* 30, R998–R1001

121 Martínez-Ara, G. *et al.* (2021) Optogenetic control of apical constriction induces synthetic morphogenesis in mammalian tissues. *bioRxiv* DOI: 10.1101/2021.04.20.440475

122 Morales-Navarrete, H. *et al.* (2019) Liquid-crystal organization of liver tissue. *Elife* 8,

123 Maroudas-Sacks, Y. *et al.* (2020) Topological defects in the nematic order of actin fibres as organization centres of Hydra morphogenesis. *Nat. Phys. 2020 172* 17, 251–259

124 Guillamat, P. *et al.* (2022) Integer topological defects organize stresses driving tissue morphogenesis. *Nat. Mater. 2022* DOI: 10.1038/S41563-022-01194-5

125 Kawaguchi, K. *et al.* (2017) Topological defects control collective dynamics in neural progenitor cell cultures. *Nat. 2017 5457654* 545, 327–331

126 Schaefer, M. *et al.* (2000) A protein complex containing Inscuteable and the Gα-binding protein Pins orients asymmetric cell divisions in Drosophila. *Curr. Biol.* 10, 353–362

127 Deforet, M. *et al.* (2014) Emergence of collective modes and tri-dimensional structures from epithelial confinement. *Nat. Commun.* 5,

128 Marin-Riera, M. *et al.* (2018) Differential tissue growth and cell adhesion alone drive early tooth morphogenesis: An ex vivo and in silico study. *PLoS Comput. Biol.* 14,

129 de Boer, B.A. *et al.* (2012) Growth of the developing mouse heart: An interactive qualitative and quantitative 3D atlas. *Dev. Biol.* 368, 203–213

130 Mao, Y. *et al.* (2013) Differential proliferation rates generate patterns of mechanical tension that orient tissue growth. *EMBO J.* 32, 2790

131 Takashima, Y. *et al.* (2012) Expansion–contraction of photoresponsive artificial muscle regulated by host–guest interactions. *Nat. Commun. 2012 31* 3, 1–8

132 Cezar, C.A. *et al.* (2016) Biologic-free mechanically induced muscle regeneration. *Proc. Natl. Acad. Sci. U. S. A.* 113, 1534–1539

133 Pan, Y. *et al.* (2016) Differential growth triggers mechanical feedback that elevates Hippo signaling. *Proc. Natl. Acad. Sci. U. S. A.* 113, E6974–E6983

134 Sunyer, R. and Trepat, X. (2020) Durotaxis. *Curr. Biol.* 30, R383–R387

135 Sunyer, R. *et al.* (2016) Collective cell durotaxis emerges from long-range intercellular force transmission. *Science (80-.).* 353, 1157–1161

136 Wen, J.H. *et al.* (2015) Haptotaxis is cell type specific and limited by substrate adhesiveness. *Cell. Mol. Bioeng.* 8, 530

137 Luo, X. *et al.* (2020) Lymphocytes perform reverse adhesive haptotaxis mediated by LFA-1 integrins. *J. Cell Sci.* 133,

138 Cheng, D. *et al.* (2019) Studies of 3D directed cell migration enabled by direct laser writing of curved wave topography. *Biofabrication* 11, 021001

139 Liao, Z. *et al.* (2021) Optogenetics-based localization of talin to the plasma membrane promotes activation of β3 integrins. *J. Biol. Chem.* 296, 100675

140 Tang, W.-C. *et al.* (2022) Optogenetic Manipulation of Cell Migration with High Spatiotemporal Resolution Using Lattice Lightsheet Microscopy. *bioRxiv* DOI: 10.1101/2022.01.02.474058

141 HA, M. *et al.* (2019) Tissue curvature and apicobasal mechanical tension imbalance instruct cancer morphogenesis. *Nature* 566, 126–130

142 Kim, S. *et al.* Harnessing mechanobiology for tissue engineering. DOI: 10.1016/j.devcel.2020.12.017

143 Bauer, A. *et al.* (2021) pyTFM: A tool for traction force and monolayer stress microscopy. *PLOS Comput. Biol.* 17, e1008364

144 Gómez-González, M. *et al.* Measuring mechanical stress in living tissues. , *Nature Reviews Physics*, 2. 01-Jun-(2020) , Springer Nature, 300–317

145 Hill, R. (1950) C. A theory of the plastic bulging of a metal diaphragm by lateral pressure. *London, Edinburgh, Dublin Philos. Mag. J. Sci.* 41, 1133–1142

146 Tambe, D.T. *et al.* (2011) Collective cell guidance by cooperative intercellular forces. *Nat. Mater. 2011 106* 10, 469–475

147 Elosegui-Artola, A. *et al.* Matrix viscoelasticity controls spatio-temporal tissue organization. DOI: 10.1101/2022.01.19.476771

148 Mason, B.N. and Reinhart-King, C.A. (2013) Controlling the mechanical properties of three-dimensional matrices via non-enzymatic collagen glycation. *http://dx.doi.org/10.4161/org.24942* 9, 70–75

149 Sarrigiannidis, S.O. *et al.* (2021) A tough act to follow: collagen hydrogel modifications to improve mechanical and growth factor loading capabilities. *Mater. Today Bio* 10, 100098

150 Bhagat, V. and Becker, M.L. (2017) Degradable Adhesives for Surgery and Tissue Engineering. *Biomacromolecules* 18, 3009–3039

Figures

Figure 1

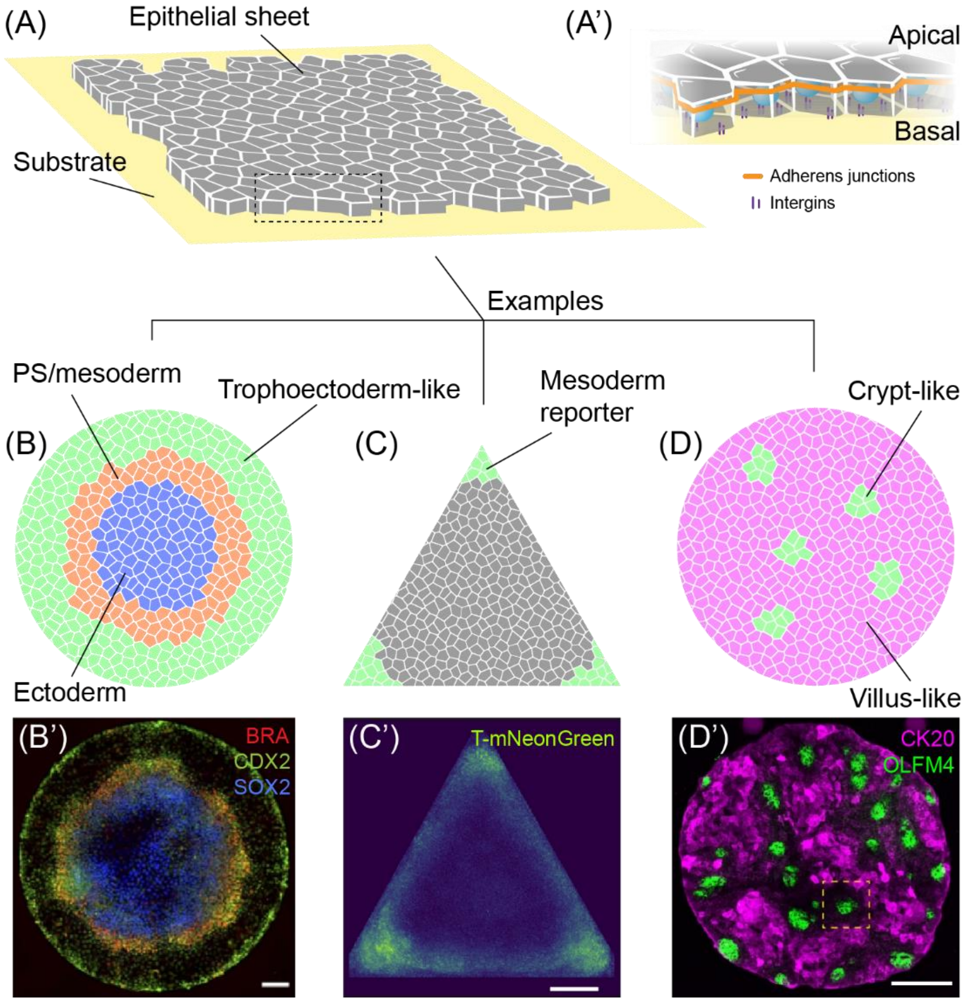

Figure 2

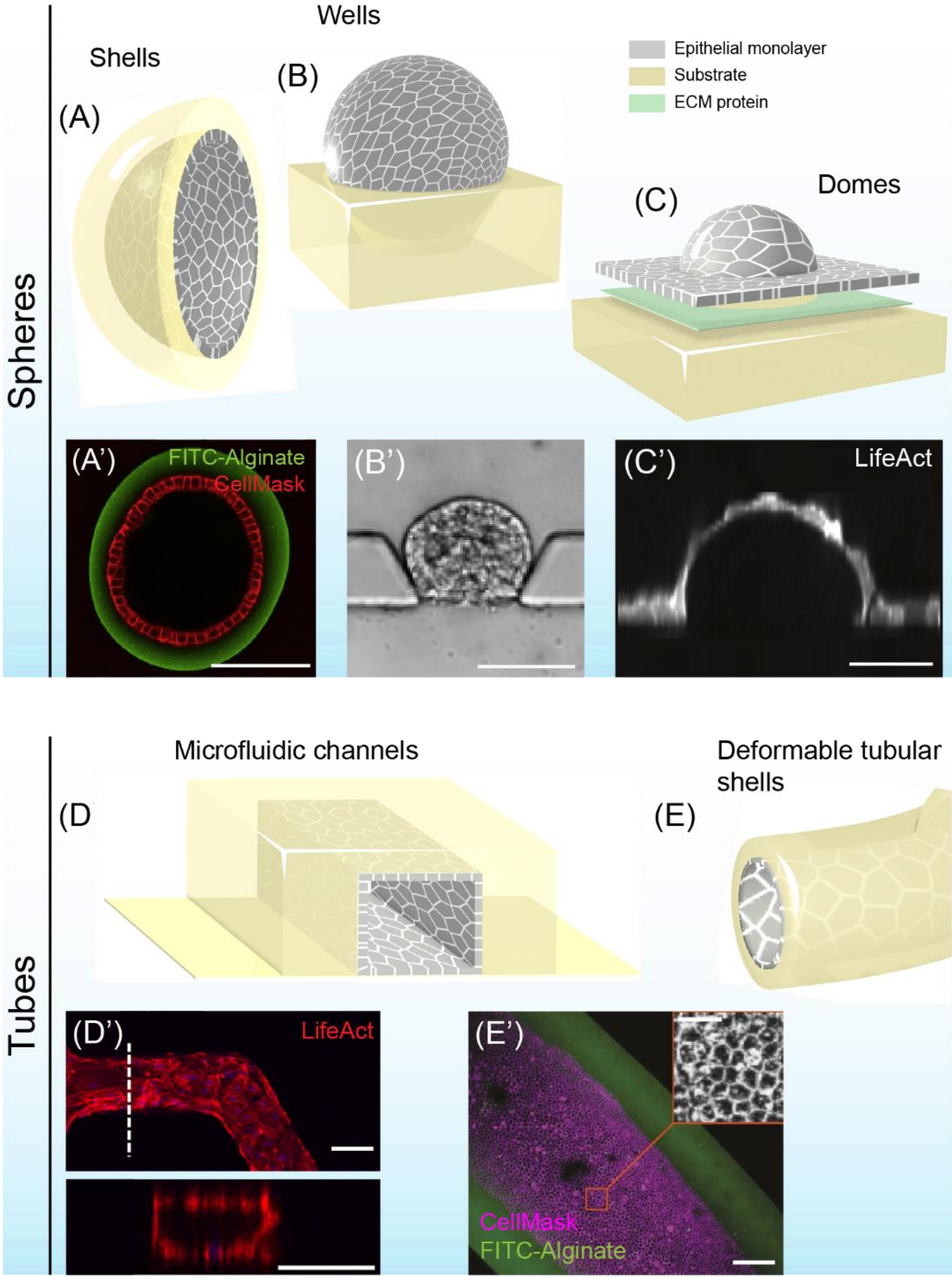

Spheres
Shells
(A)
Wells
(B)
Epithelial monolayer
Substrate
ECM protein
(C)
Domes
(A')
FITC-Alginate
CellMask
(B')
(C')
LifeAct
Tubes
Microfluidic channels
(D
Deformable tubular shells
(E)
(D')
LifeAct
(E')
CellMask
FITC-Alginate

Figure 3

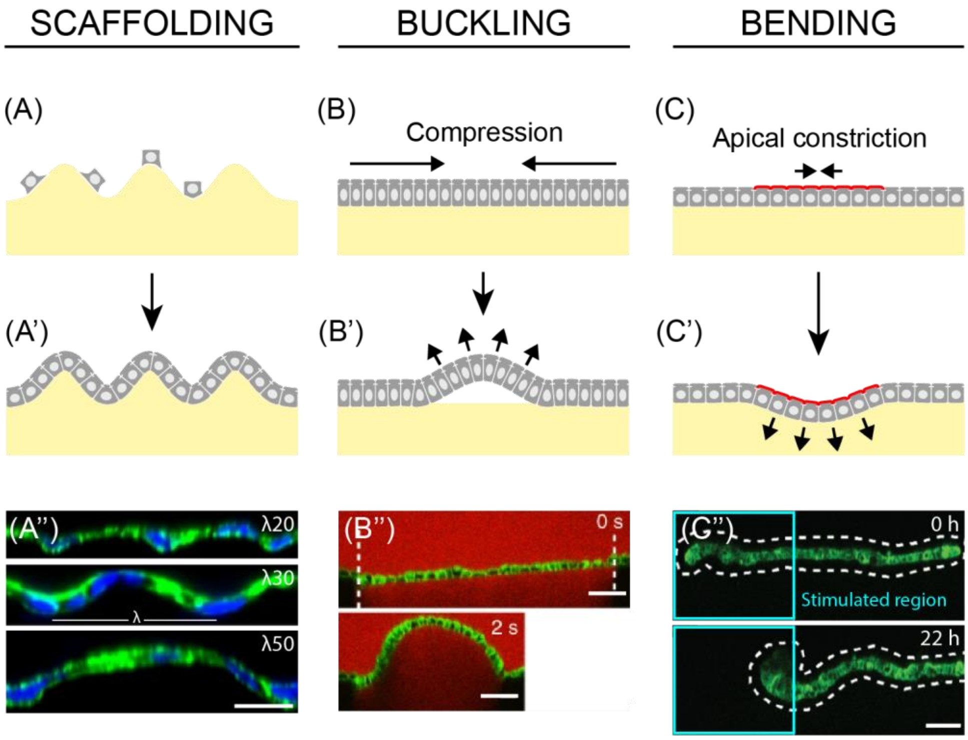

SCAFFOLDING
BUCKLING
BENDING
(A)
(B)
Compression
(C)
Apical constriction
(A')
(B')
(C')
(A")
λ20
λ30
λ
λ50
(B")
0 s
2 s
(C")
0 h
Stimulated region
22 h

Figure 4

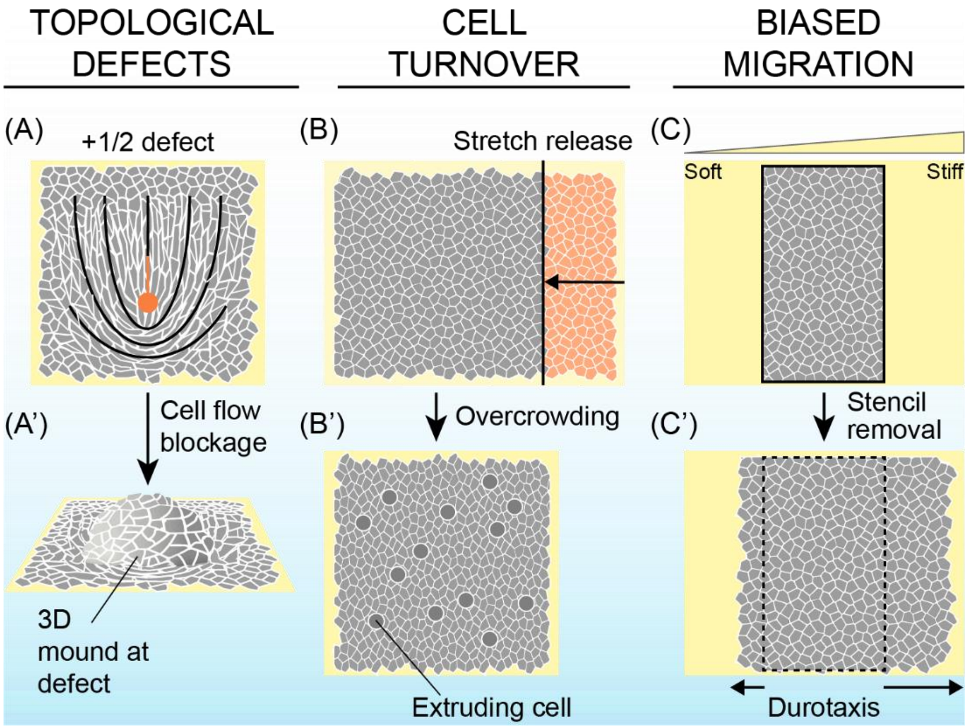
TOPOLOGICAL DEFECTS
CELL TURNOVER
BIASED MIGRATION
(A)
+1/2 defect
(B)
Stretch release
(C)
Soft
Stiff
(A')
Cell flow blockage
(B')
Overcrowding
(C')
Stencil removal
3D mound at defect
Extruding cell
Durotaxis

Figure I

(A)

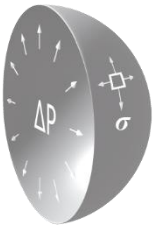

(B)